Macromolecules

Article

pubs.acs.org/Macromolecules

A New Pentacyclic Indacenodiselenophene Arene and Its Donor–Acceptor Copolymers for Solution-Processable Polymer Solar Cells and Transistors: Synthesis, Characterization, and Investigation of Alkyl/Alkoxy Side-Chain Effect

Huan-Hsuan Chang, Che-En Tsai, Yu-Ying Lai, Wei-Wei Liang, So-Lin Hsu, Chain-Shu Hsu, and Yen-Ju Cheng*

Department of Applied Chemistry, National Chiao Tung University, 1001 Ta Hsueh Road, Hsin-Chu, 30010 Taiwan

Supporting Information

ABSTRACT: A pentacyclic indacenodiselenophene (IDS) arene was synthesized via intramolecular Friedel-Craft cyclization of the selenophene moieties. This IDS framework was used as a model system to investigate the alkyl/alkoxy side-chain effect by preparing **IDS-OCH$_8$** and **IDS-C$_6$**, where the side chains on the sp^3 carbon in the cyclopentadienyl ring are 4-octyloxyphenyl groups and 4-hexylphenyl groups, respectively. The **Sn-IDS-OCH$_8$** and **Sn-IDS-C$_6$** monomers were copolymerized with 4,7-dibromo-2,1,3-benzothiadiazole (**BT**), 4,7-diiodo-5,6-difluoro-2,1,3-benzothiadiazole (**FBT**) and 1,3-dibromothieno[3,4-*c*]pyrrole-4,6-dione (**TPD**) acceptor monomers by Stille polycondensation to afford five new IDS-based donor–acceptor alternating copolymers, **PIDSBT-OCH$_8$**, **PIDSBT-C$_6$**, **PIDSFBT-OCH$_8$**, **PIDSFBT-C$_6$**, and **PIDSTPD-C$_6$**. Despite the fact that the octyloxy and hexyl side chains play a negligible role in the optical and electrochemical properties of the resulting polymers, the solar cell performance is highly associated with the side chains of the polymers. Under similar device fabrication conditions, the **PIDSBT-C$_6$** and **PIDSFBT-C$_6$**-based devices showed much improved efficiencies than the corresponding **PIDSBT-OCH$_8$**, and **PIDSFBT-OCH$_8$**-based devices (2.6% and 1.9% vs 3.8% and 3.9%). The improvement is mainly the result of much enhanced J_{sc} values. Consistently, **PIDSBT-C$_6$** and **PIDSFBT-C$_6$** exhibited much higher FET hole mobilites than the corresponding **PIDSBT-OCH$_8$**, and **PIDSFBT-OCH$_8$**. These results clearly revealed that the 4-hexylphenyl group is a more suitable side chain than the 4-octyloxyphenyl group in the IDS system, and the side-chain dependent mobility of the polymers is the dominating factor to determine the photocurrents and efficiencies of PSCs. **PIDSBT-C$_6$** exhibited a high hole mobility of 0.08 cm^2 V^{-1} s^{-1} and **PIDSTPD-C$_6$**:PC$_{71}$BM (1:4 in wt %)-based solar cell with 5 v% chloronaphthalene (CN) delivered a V_{oc} of 0.92 V, a J_{sc} of 9.77 mA/cm^2, an FF of 51%, and a highest PCE of 4.6%. This work not only discloses a new selenophene-containing ladder-type IDS structure and its copolymers but also provides useful insights into the alkyl/alkoxy side-chain effect for future design of conjugated polymers.

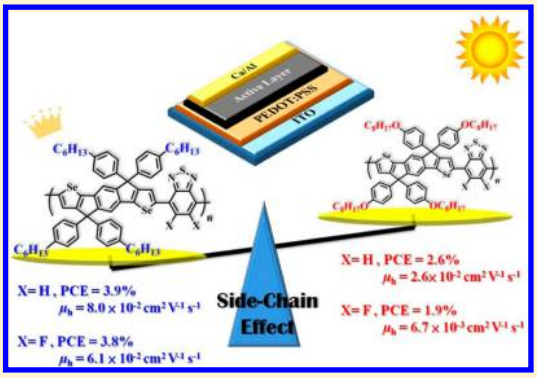

INTRODUCTION

Polymer solar cells (PSCs) using organic p-type (donor) and n-type (acceptor) semiconductors have attracted tremendous scientific and industrial interest.[1] The most critical challenge at molecular level is to develop p-type conjugated polymers that can simultaneously possess sufficient solubility for processability and miscibility with an n-type material, low band gap (LBG) for strong and broad absorption spectrum to capture more solar photons, and high hole mobility for efficient charge transport.[2] The most useful approach to make a LBG polymer is to connect electron-rich donor and electron-deficient acceptor segments along the conjugated polymer backbone. Benzene and thiophene aromatic rings are the most important ingredients to comprise p-type conjugated polymers, considering that the benzene-containing polymers having lower-lying HOMO energy levels can acquire higher V_{oc},[3] and the thiophene-containing polymers with broader absorption can yield better J_{sc}.[4] On the other hand, the ladder-type conjugated architectures have attracted growing research interest for PSC applications.[5] Forced planarization by covalently fastening adjacent aromatic units in the polymer backbone elongates effective conjugation length, facilitates π-electron delocalization, and enhances the intrinsic charge mobility.[6] Integration of thiophene and benzene into a single molecular entity with a fused and elongated conjugated structure has led to a series of fascinating conjugated molecules.[7] Selenophene is an analogue of thiophene with selenium replacing the sulfur atom. Selenophene and its polymers have several potential advantages over the thiophene counterparts and attracted considerable interest for the applications in PSCs.[8] Theoretical calculations

Received: July 9, 2013
Revised: September 3, 2013
Published: September 19, 2013

 © 2013 American Chemical Society

reveal that polyselenophenes have a more quinoidal character and less tendency of twisting.[9] Heeney and co-workers reported that poly(3-hexylselenophene) has a smaller band gap of 1.6 eV than P3HT through lowering the LUMO level without elevating the HOMO level.[10] These are promising properties for obtaining profound absorption at lower energy while maintaining a comparable open-circuit voltage. It was also found that P3HS is more resistant to photo-oxidation than P3HT due to the low-lying LUMO of P3HS and the smaller ionization potential of selenium.[10] Furthermore, selenium is more polarizable than sulfur, which might induce intermolecular Se−Se interaction to improve the charge carrier mobility.[11] However, compared with the thiophene analogues, research on selenophene-containing polymers is relatively scarce owing to less explored chemistry and more difficult functionalization of selenophene. In this research, for the first time, we have designed and synthesized a new selenophene-based pentacyclic molecule, indacenodiselenophene (IDS), where the central phenylene ring is fused with two outer selenophenes by carbon bridges (Figure 1).

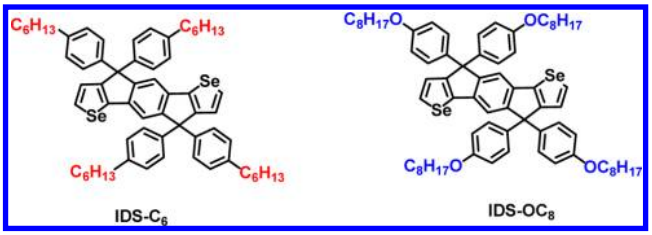

Figure 1. Chemical structures of pentacyclic **IDS-C$_6$** and **IDS-OCH$_8$**.

Side-chain engineering has been demonstrated to play a critical role in optimizing the molecular properties of D−A copolymers. The length, branch and rigidity of the side-chains, as well as the position of attachment on the conjugated frameworks would dramatically influence the solubility, crystallization, and molecular packing.[12] These microscopic molecular modification could significantly change the macroscopic parameters of the device performance. Alkyl or alkoxy moieties are widely used as the side chains attached on the conjugated backbones for PSCs.[13] From a synthetic viewpoint, introducing alkoxy side-chain into a conjugated system via a simple S_N2 *O*-alkylation seems to be more practical. Nevertheless, systematic investigation and comparison of the effect of alkyl/alkoxy substitutions on the molecular properties of a given conjugated polymer are insufficient. Very recently, Jen and Cheng independently reported an indacenodithieno[3, 2-*b*]thiophene (**IDTT**)-based donor−acceptor copolymer (**PIDTTFBT**) with an identical conjugated backbone but different side chains on the **IDTT** units (4-octyloxyphenyl vs 4-hexylphenyl groups).[14] Such a structural variation indeed made a difference in efficiency of the PSCs.[14] We envisage that the newly developed indacenodiselenophene unit could serve as a model system to investigate the alkyl/alkoxy side-chain effect and shed light on the future molecular design for side-chain engineering. In this regard, we have successfully prepared two IDS-based units, **IDS-OCH$_8$** and **IDS-C$_6$**, where the two side-chains on the sp^3 carbon in the cyclopentadienyl ring are 4-octyloxyphenyl groups and 4-hexylphenyl groups, respectively (Figure 1). These IDS units were copolymerized with 4,7-diiodo-2,1,3-benzothiadiazole (**BT**), 4,7-dibromo-5,6-difluoro-2,1,3-benzothiadiazole (**FBT**), and 1,3-dibromothieno[3,4-*c*]-pyrrole-4,6-dione (**TPD**) acceptor monomers to afford a series of new IDS-based donor−acceptor alternating copolymers, **PIDSBT-OCH$_8$**, **PIDSBT-C$_6$**, **PIDSFBT-OCH$_8$**, **PIDSFBT-C$_6$**, and **PIDSTPD-C$_6$** (Figure 2). Their synthesis, molecular properties and applications in solution-processable PSCs as well as organic transistors will be reported and discussed.

RESULTS AND DISCUSSION

Synthesis. The synthetic route for **Sn-IDS-OCH$_8$** monomer is depicted in Scheme 1. Stille coupling of diethyl 2,5-dibromoterephthate with 2-(tributylstannyl)selenophene yielded compound **1**. Double nucleophilic addition of the ester groups in **1** by (4-octyloxy)phenylmagnesium bromide led to the formation of benzylic alcohols in **2** which was subjected to intramolecular Friedel−Crafts cyclization under acidic conditions to furnish the pentacyclic **IDS-OCH$_8$** arene in a good yield of 73%. This is also the first example demonstrating that a selenophene moiety can efficiently undergo Friedel−Crafts cyclization at its 3-position. Finally, **IDS-OCH$_8$** was lithiated by *n*-butyllithium followed by quenching with

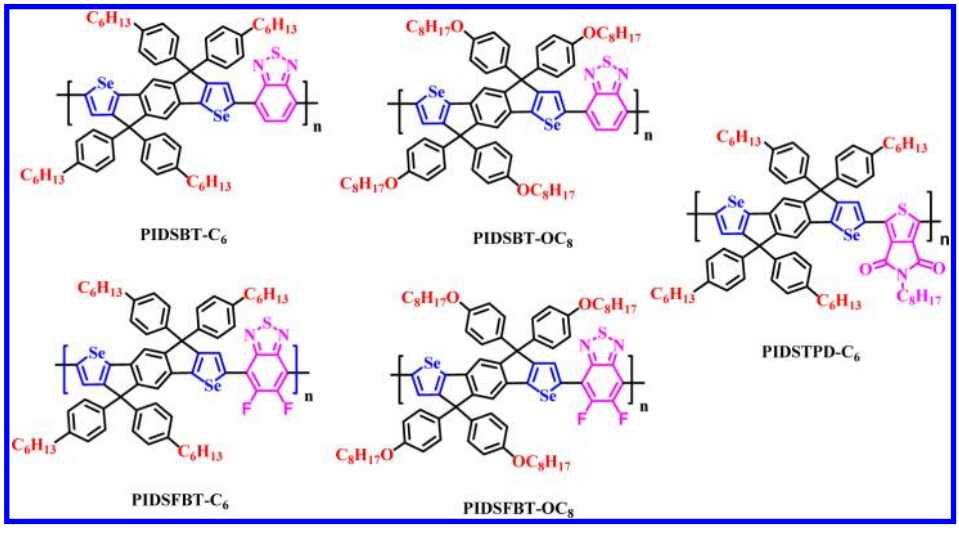

Figure 2. Chemical structures of **IDS-OCH$_8$**- and **IDS-C$_6$**-based donor−acceptor copolymers **PIDSBT-OCH$_8$**, **PIDSBT-C$_6$**, **PIDSFBT-OCH$_8$**, **PIDSFBT-C$_6$**, and **PIDSTPD-C$_6$**.

dx.doi.org/10.1021/ma401415g | *Macromolecules* 2013, 46, 7715−7726

Scheme 1. Synthetic Route for Sn-IDS-C_6 and Sn-IDS-OCH_8

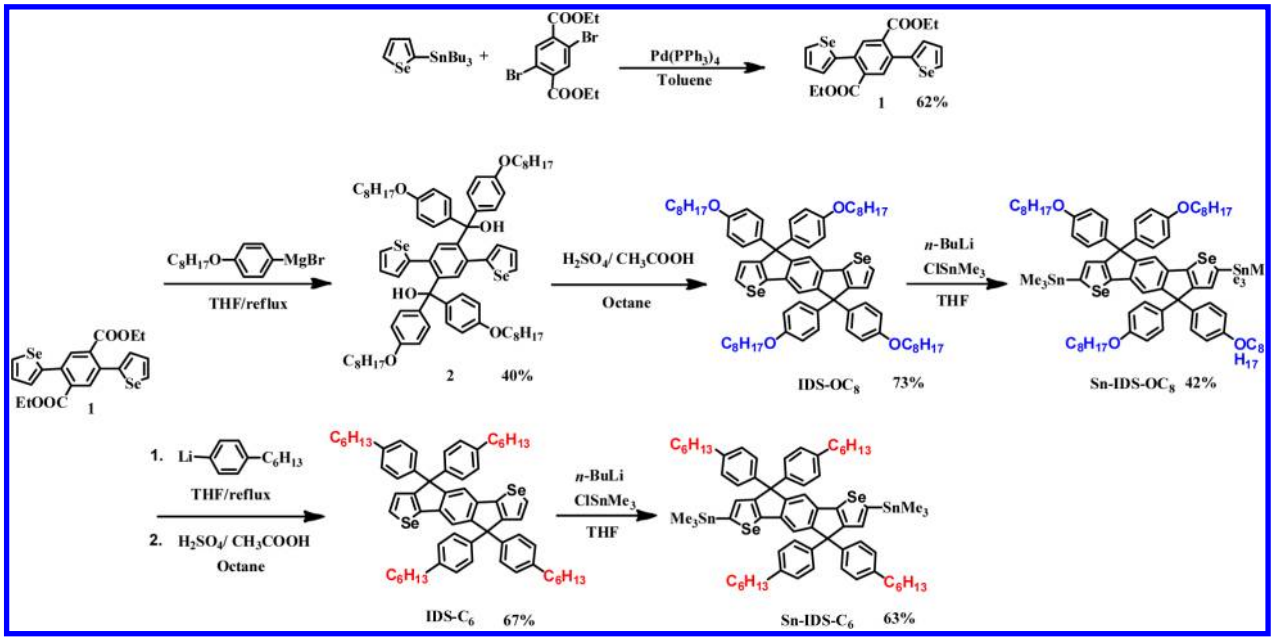

trimethyltin chloride to afford the distannyl **Sn-IDS-OCH_8** in a moderate yield of 42%. The **Sn-IDS-C_6** monomer was also synthesized in a similar manner. The difference is that compound **1** was reacted with 4-hexylphenyllithium to give the corresponding alcohol intermediate, which subsequently underwent acid-mediated intramolecular annulation reaction to furnish **IDS-C_6** in one pot. **Sn-IDS-OCH_8** and **Sn-IDS-C_6** monomers were copolymerized with 4,7-dibromo-2,1,3-benzothiadiazole (**BT**), 4,7-diiodo-5,6-difluoro-2,1,3-benzothiadiazole (**FBT**), and 1,3-dibromothieno[3,4-*c*]pyrrole-4,6-dione (**TPD**) acceptor monomers via Stille polycondensation to afford a range of donor−acceptor copolymers, **PIDSBT-OCH_8**, **PIDSBT-C_6**, **PIDSFBT-OCH_8**, **PIDSFBT-C_6**, and **PIDSTPD-C_6**, respectively (Scheme 2). These copolymers

Scheme 2. Stille Coupling Polymerization leading to IDS-Based Donor−Acceptor Copolymers

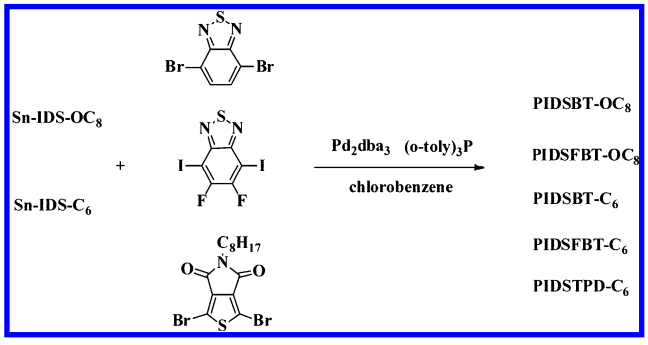

purified by successive Soxhlet extraction and precipitation showed narrow polydispersity index. Controlling the molecular weights of **PIDSBT-OCH_8** (10.7 KDa) and **PIDSBT-C_6** (10.8 KDa), as well as **PIDSFBT-OCH_8** (11.5 KDa) and **PIDSFBT-C_6** (9.3 KDa) to be similar allows us to make the head-to-head comparison of the side-chain effects on the molecular properties appropriately. The resultant copolymers flanked with four side chains on the **IDS** unit possess excellent solubility in common organic solvents, such as chloroform, toluene, and THF. The determination of molecular weight for **PIDSTPD-C_6** was not successful owing to the fact that it has very poor solubility in THF. However, as can be deduced from the poor solubility of PIDSTPD-C_6 in THF, PIDSTPD-C_6 may possess much higher molecular weight than the other four polymers.

Thermal and Optical Properties. The thermal stability of the polymers was analyzed by thermogravimetric analysis (TGA) (Figure 3). **PIDSBT-OCH8**, **PIDSFBT-OCH8**,

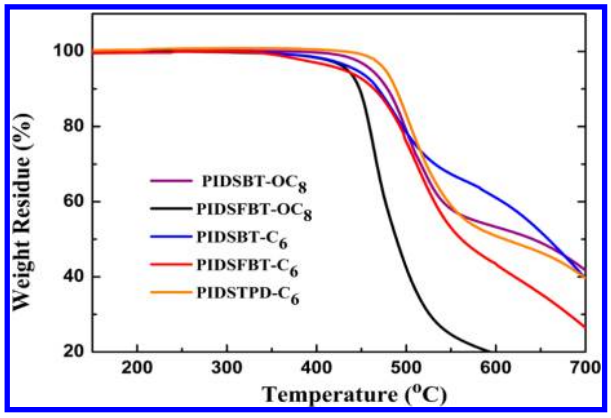

Figure 3. Thermogravimetric analysis (TGA) of the IDS-based copolymers.

PIDSBT-C6, **PIDSFBT-C6**, and **PIDSTPD-C6** exhibited sufficiently high decomposition temperatures (T_d) of 460, 434, 444, 430, and 477 °C, respectively. The DSC measurements showed no thermal transitions, implying their amorphous nature.

UV−vis absorption spectra of the five polymers in THF solutions and in thin films are shown in Figure 4 and the correlated optical parameters are summarized in Table 1. **PIDSBT-OCH_8**, **PIDSFBT-OCH_8**, **PIDSBT-C_6**, and **PIDSFBT-C_6** showed two obvious absorption bands in the spectra. The longer wavelength absorbance is attributed to the intramolecular charge transfer (ICT) between the electron-rich

dx.doi.org/10.1021/ma401415g | *Macromolecules* 2013, 46, 7715−7726

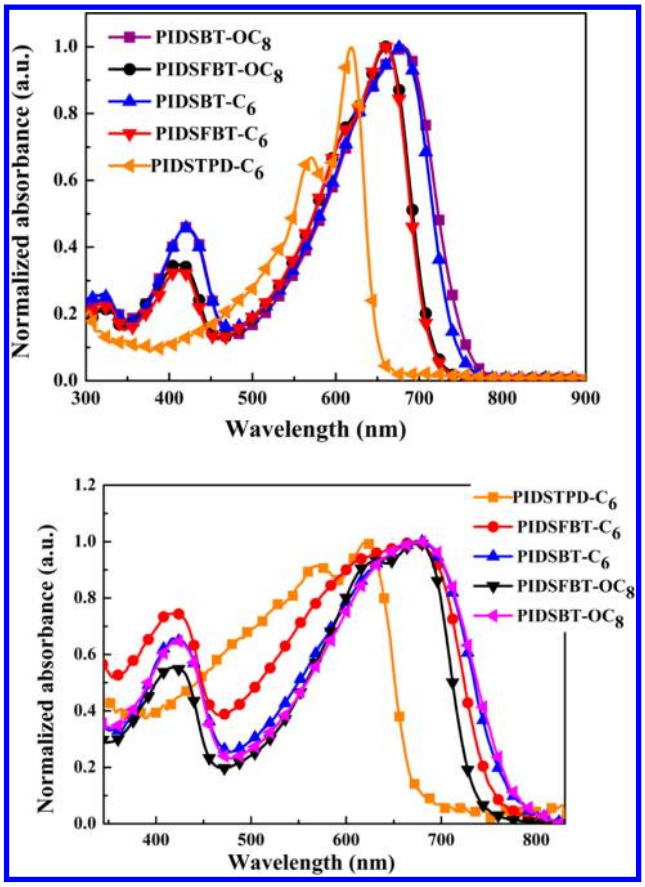

Figure 4. Normalized absorption spectra of **PIDSBT-OCH$_8$**, **PIDSFBT-OCH$_8$**, **PIDSBT-C$_6$**, **PIDSFBT-C$_6$**, and **PIDSTPD-C$_6$** in (a) THF solutions and (b) in thin films.

and the electron-deficient segments. However, the localized transition bands and ICT bands for **PIDSTPD-C$_6$** are overlapped into a broad band covering the whole visible region from 400 to 700 nm, indicating that the accepting strength of **TPD** is weaker than that of **BT** and **FBT** units. The absorption profiles of the five polymers shift toward longer wavelengths from the solution state to the solid state. The optical band gaps (E_g^{opt}) deduced from the onset of absorption in the solid state are determined to be 1.60 eV for **PIDSBT-OCH$_8$** and **PIDSBT-C$_6$**, 1.68 eV for **PIDSFBT-OCH$_8$**, 1.63 eV for **PIDSFBT-C$_6$**, and 1.84 eV for **PIDSTPD-C$_6$**. These results indicate that 4-octyloxyphenyl and 4-hexylphenyl side chains have negligible effect on the optical properties of the polymers.

Electrochemical Properties. Cyclic voltammetry (CV) was employed to examine the electrochemical properties and determine the highest occupied molecular orbital (HOMO) and lowest unoccupied molecular orbital (LUMO) energies of the polymers (Figure 5, Table 1). The polymers showed stable

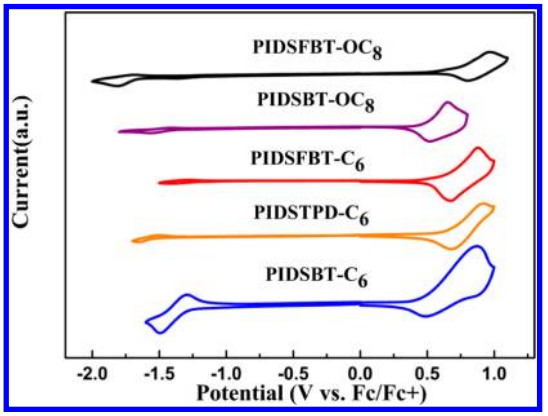

Figure 5. Cyclic voltammograms of **PIDSBT-OCH$_8$**, **PIDSFBT-OCH$_8$**, **PIDSBT-C$_6$**, **PIDSFBT-C$_6$**, and **PIDSTPD-C$_6$** in the thin films at a scan rate of 50 mV/s.

and reversible p-doping and n-doping processes, which are important prerequisites for p-type semiconductor materials. The LUMO energy levels of **PIDSBT-OCH$_8$**, **PIDSBT-C$_6$**, **PIDSFBT-OCH$_8$**, **PIDSFBT-C$_6$**, and **PIDSTPD-C$_6$** are determined to be −3.45, −3.51, −3.57, −3.61, and −3.28 eV, respectively. The LUMO energy levels are higher than that of the PC$_{71}$BM acceptor (−3.8 eV) to ensure energetically favorable electron transfer. It should be noted that the HOMO energy of fluorinated **PIDSFBT-OCH$_8$** (−5.32 eV), **PIDSFBT-C$_6$** (−5.38 eV) is lower than that of the corresponding nonfluorinated **PIDSBT-OCH$_8$** (−5.28 eV), **PIDSBT-C$_6$** (−5.28 eV) due to the two electron-withdrawing fluorine atoms on the **BT** units.[15] Furthermore, **PIDSTPD-C$_6$** showed the deepest HOMO energy level of −5.43 eV. The HOMO energy levels are within the ideal range to ensure good air-stability and large attainable V_{oc}. Again, we did not observe the significant impact of OC$_8$/C$_6$ substituents on the electrochemical properties of the polymers. The conjugation backbones of the polymers predominate in determining their E_{HOMO} and E_{LUMO}.

Photovoltaic Characteristics. Bulk heterojunction photovoltaic cells were fabricated by spin-coating the blends from *ortho*-dichlorobenzene solutions at various polymer-to-PC$_{71}$BM ratios on the basis of ITO/PEDOT:PSS/polymer:PC$_{71}$BM/

Table 1. Summary of the Intrinsic Properties of the Polymers

					λ_{max} (nm)			
polymer	M_n (kDa)	PDI	T_d (°C)	E_g^{opt} (eV) (film)	THF	film	E_{HOMO} (eV)	E_{LUMO} (eV)
PIDSBT-OCH$_8$	10.7	1.7	460	1.60	420 678	422 682	−5.28	−3.45
PIDSBT-C$_6$	10.8	2.0	444	1.60	420 678	418 680	−5.28	−3.51
PIDSFBT-OCH$_8$	11.5	1.7	434	1.68	414 660	418 672	−5.32	−3.57
PIDSFBT-C$_6$	9.3	1.6	430	1.63	410 660	418 676	−5.38	−3.61
PIDSTPD-C$_6$	–	–	477	1.84	617	621	−5.43	−3.28

dx.doi.org/10.1021/ma401415g | *Macromolecules* 2013, 46, 7715−7726

Ca/Al configuration and their performances were measured under a simulated AM 1.5 G illumination of 100 mW/cm^2. The characterization data are summarized in Table 2 and the $J-V$

Table 2. Summary of Device Parameters

polymer	blend ratio polymer:$PC_{71}BM$	V_{oc} (V)	J_{sc} (mA/cm^2)	FF (%)	PCE (%)
PIDSBT-OCH$_8$	1:4	0.76	8.45	41	2.6
PIDSBT-C$_6$	1:4	0.76	11.24	45	3.9
PIDSFBT-OCH$_8$	1:3	0.86	6.72	32	1.9
PIDSFBT-C$_6$	1:3	0.84	9.67	47	3.8
PIDSTPD-C$_6$	1:4	0.92	7.96	51	3.8
PIDSTPD-C$_6$ with 5 vol % CN	1:4	0.92	9.77	50	4.6

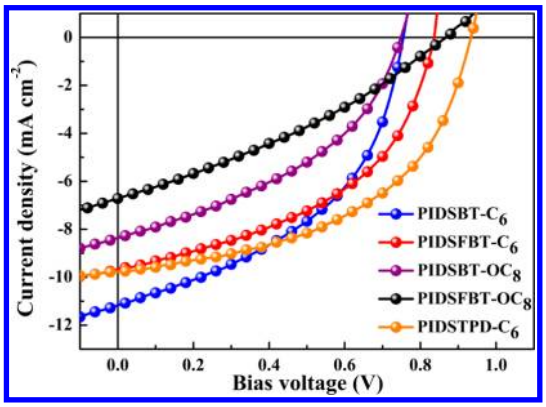

Figure 6. $J-V$ characteristics of ITO/PEDOT:PSS/IDS-based polymers:$PC_{71}BM$/Ca/Al under illumination of AM1.5, 100 mW/cm^2.

curves of these polymers are shown in Figure 6. The blend ratio of the active layers shown in the Table 2 is the result of the optimized conditions for the devices. The device based on the **PIDSBT-OCH$_8$**:$PC_{71}BM$ (1:4 in wt %) blend exhibited a V_{oc} of 0.76 V, a J_{sc} of 8.45 mA/cm^2, an FF of 41%, delivering a moderate PCE of 2.6%. However, the device based on the **PIDSBT-C$_6$**:$PC_{71}BM$ (1:4 in wt %) blend exhibited a V_{oc} of 0.76 V, a high J_{sc} of 11.24 mA/cm^2, an FF of 45%, leading to a much improved PCE of 3.9% by 1.5-fold. Meanwhile, the device using **PIDSFBT-OCH$_8$**:$PC_{71}BM$ (1:3 in wt %) blend exhibited a V_{oc} value of 0.86 V, a J_{sc} of 6.72 mA/cm^2 with a PCE of 1.9%. With the same blend ratio, **PIDSFBT-C$_6$**:$PC_{71}BM$ (1:3 in wt %) blend exhibited a V_{oc} value of 0.84 V and a greater J_{sc} of 9.67 mA/cm^2 with a PCE to 3.8%, which represents a 2-fold improvement. The head-to-head comparison in the two cases clearly indicates that the polymers with the 4-hexylphenyl side-chains yielded much better performance than their corresponding counterparts with the 4-octyloxyphenyl side chains. The improvement is mainly the result of enhanced J_{sc} values. Considering that the C_6 and OC_8 have little influence on the optical and electrochemical properties, the discrepancy is presumably ascribed to the different steric effect of the side chains, resulting in different molecular packing and morphology in the binary composites. Furthermore, the devices with fluorinated polymers showed higher V_{oc} values which are attributed to the lower-lying of HOMO energy levels due to the fluorine withdrawing effect. Because of the fact that the hexyl group is superior to the octyloxy in the IDS system, we further synthesized **PIDSTPD-C$_6$** copolymer using TPD unit as the acceptor comonomer and 4-hexylphenyl group as the side chain. **PIDSTPD-C$_6$**:$PC_{71}BM$ (1:4 in wt %)-based device exhibited a highest V_{oc} of 0.92 V, a J_{sc} of 7.96 mA/cm^2, an FF of 51%, and a PCE of 3.8%. By adding 5 v% chloronaphthalene (CN) to optimize the morphology, the J_{sc} of the devices increased from 7.96 mA/cm^2 to 9.77 mA/cm^2, and the PCE improved from 3.8% to 4.6%.

Organic Field Effect Transistors. To investigate the mobilities of the polymers, organic field-effect transistors (OFETs) were fabricated in the bottom-gate/top-contact geometry as described in the Experimental Section (Table 3 and Figure 7). The hole mobilities were deduced from the transfer characteristics of the devices in the saturation regime. The polymers-based OFETs using SiO_2 as gate dielectric were treated with octadecyltrichlorosilane (ODTS) to form a self-assembly monolayer (SAM) and thermally annealed at 120 or 200 °C. All of the selenophene-based copolymers delivered decent hole mobilites in the range around $10^{-1}-10^{-2}$ cm^2 V^{-1} s^{-1}. **PIDSBT-C$_6$** exhibited higher hole mobility of 8.0×10^{-2} cm^2 V^{-1} s^{-1} than **PIDSBT-OCH$_8$** with 2.6×10^{-2} cm^2 V^{-1} s^{-1}. Meanwhile, **PIDSFBT-C$_6$** also showed higher hole mobility than **PIDSFBT-OCH$_8$** by almost 1 order of magnitude (6.1×10^{-2} cm^2 V^{-1} vs 6.7×10^{-3} cm^2 V^{-1}). The trend of FET mobilities is in good agreement with the efficiencies in the PSCs, suggesting that the intrinsic mobility of the polymers is the dominating factor to determine the solar cell performance. This result again indicates that the side-chain effect is important, and the 4-hexylphenyl group is better than the 4-oxyloxyphenyl groups in the IDS conjugated system.

Theoretical Calculations. *Electronic effect.* In order to investigate the intrinsic difference between the alkyl and alkoxy groups in the polymers, the pair of **PIDSBT-OCH$_8$** and **PIDSBT-C$_6$** polymers was chosen to compare their optical and electronic characteristics by computation. Considering an insignificant effect on electronic properties, all the aliphatic substituents were replaced with methyl groups for simplicity. Dimeric repeating units, denoted as **2IDSBT-OCH$_3$** and **2IDSBT-CH$_3$**, were then selected as the model compounds. PM6 was employed as the geometry optimization method on account of the fact that it is computationally less demanding than DFT methods but with reasonable accuracy for geometry.[16] Subsequently, the optimized geometries were used in the time-dependent density functional calculations

Table 3. FET Characteristics of the Polymer Thin Films

polymer	SAM layer	annealing temperature (°C)	mobility (cm^2 V^{-1} s^{-1})	on/off	V_t (V)
PIDSBT-OCH$_8$	ODTS	200	2.6×10^{-2}	4.1×10^1	−2.09
PIDSBT-C$_6$	ODTS	200	8.0×10^{-2}	3.5×10^3	−15.99
PIDSFBT-OCH$_8$	ODTS	200	6.7×10^{-3}	2.8×10^4	−17.98
PIDSFBT-C$_6$	ODTS	200	6.1×10^{-2}	9.7×10^2	−15.72
PIDSTPD-C$_6$	ODTS	120	2.0×10^{-2}	5.1×10^2	−1.68

dx.doi.org/10.1021/ma401415g | Macromolecules 2013, 46, 7715−7726

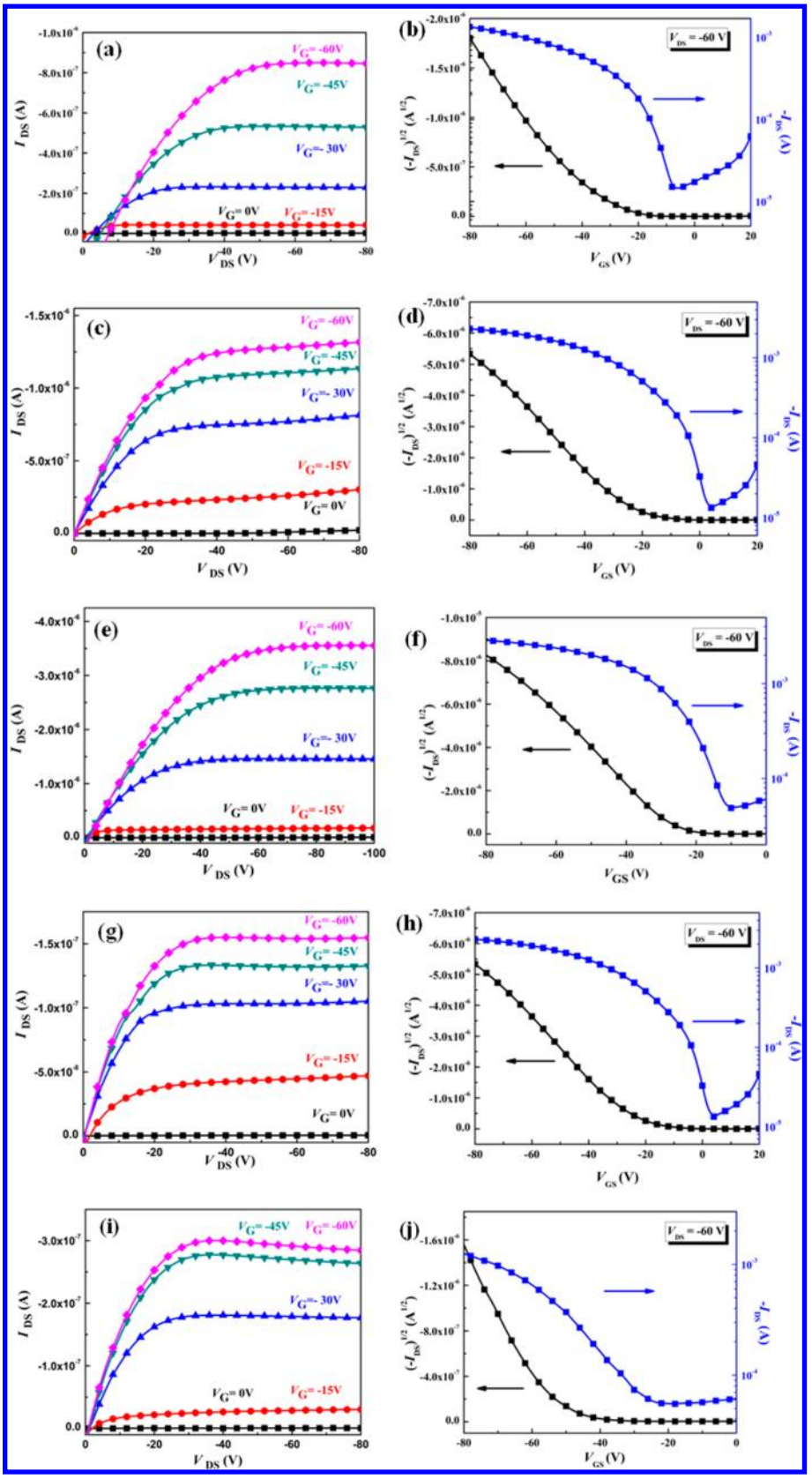

Figure 7. Typical output curves (a, c, e, g, i) and transfer plots (b, d, f, h, j) of the OFET devices based on **PIDSBT-OCH$_8$**, **PIDSFBT-OCH$_8$**, **PIDSBT-C$_6$**, and **PIDSFBT-C$_6$** **PIDSTPD-C$_6$**, respectively, with the ODTS-SAM layer.

(TD-B3LYP/6-311G(d,p)) with solvation in THF by applying the polarized continuum model (PCM) to estimate their optical and electronic properties. The calculated HOMO/LUMO energy, excitation energy, oscillator strength, and configurations of the excited states are summarized in Table 4 and the frontier orbitals, HOMO and LUMO are illustrated

dx.doi.org/10.1021/ma401415g | *Macromolecules* 2013, 46, 7715−7726

Table 4. Calculated[a] HOMO/LUMO Energy, Excitation Energy, Oscillator Strength, and Configurations (with Large CI Coefficients) of the Excited States

			excitation energy				
compound	HOMO (eV)	LUMO (eV)	$\lambda_{max,exp}$ (nm)[b]	λ_{calcd} (nm)	oscillator strength	symmetry	configuration[c]
2IDSBT-OCH_3	−5.22	−2.83	678	634	0.4831	singlet-A	**H → l**
			420	425	0.291	singlet-A	**H−8 → L**; H−6 → L
							H−10 → L; H−9 → L
							H−5 → L; H−4 → L + 1
							H → L + 2
				415	1.1626	singlet-A	H−9 → L; H−1 → L + 3
							H → L + 2; H−7 → L
							H−6 → L; H−1 → L + 2
2IDSBT-CH_3	−5.26	−2.84	678	625	0.4282	singlet-A	**H → L**
			420	414	1.3345	singlet-A	H−2 → L; H−1 → L + 3
							H → L + 2; H−1 → L + 2
				409	0.4391	singlet-A	**H−2 → L**; H → L + 2
							H−8 → L; H−6 → L
							H−5 → L; H−4 → L
							H−1 → L + 2; H−1 → L + 3

[a]TD-B3LYP/6-311G(d,p), PCM=THF. [b]Experimental values were measured for nonsimplified **PIDSBT-OCH_8** and **PIDSBT-C_6** in the THF solution. [c]Configurations with largest coefficients in the CI expansion of each state are highlighted in boldface.

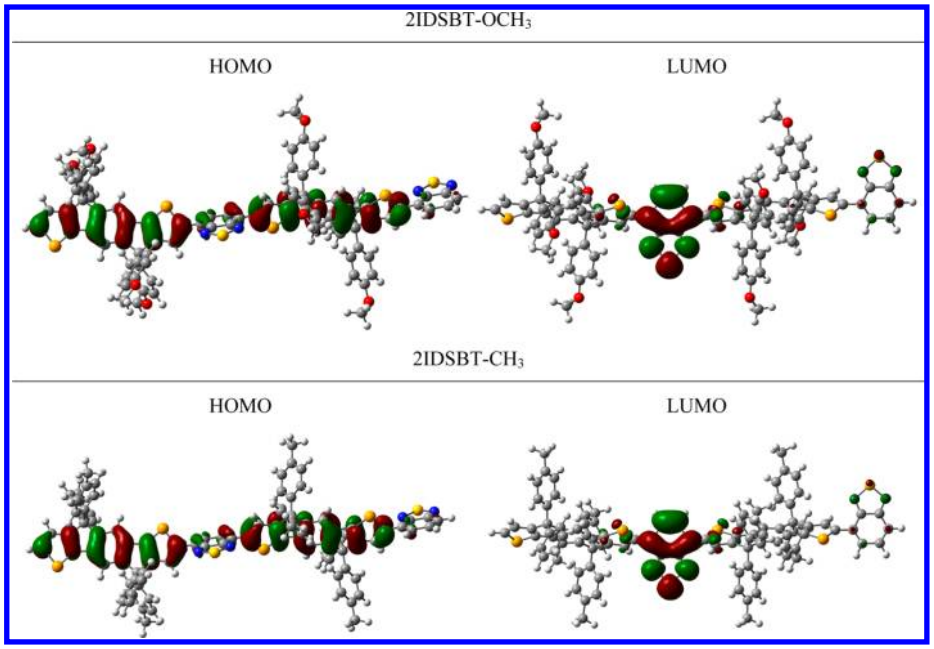

Figure 8. Plots (isovalue = 0.02 au) of frontier orbitals of **2IDSBT-OCH_3** and **2IDSBT-CH_3**, calculated at the level of B3LYP/6-311G(d,P) in THF.

in Figure 8. In spite of variations in the absolute values, the calculated absorptions are still in good agreement with the experimental values. For **2IDSBT-OCH_3** and **2IDSBT-CH_3**, their calculated HOMO/LUMO energy levels (Table 4) are fairly close and the orbital electron density distributions (Figure 8) are similar to each other, and so do the calculated absorption bands. The computational results are consistent with the electrochemical and optical measurements, supporting the argument that the alkyl and alkoxy substituents have insignificant impact on the electronic properties of the polymers. The presence of the bridging sp^3-carbon hinders the orbital communication between the alkoxyphenyl/alkylphenyl side chains and the polymeric conjugated backbone, thus resulting in trivial electronic disparity between these polymers.

Steric Effect. Since the alkyl and alkoxy groups have negligible influence on the electronic properties of the polymers, the discrepancy observed in PSCs and OFETs might be ascribed to the steric effect of the side chains, leading to different intermolecular interaction and packing in the solid state. **IDS-C_6** and **IDS-OCH_8** were selected as the model compounds to theoretically examine the steric relationship of the alkyl/alkoxy substituent with the molecular main chain. The optimized structures of **IDS-C_6** and **IDS-OCH_8** calculated by PM6 are illustrated in Figure 9. The backbones of C_6 and OC_8 are aligned with a zigzag conformation within a plane. For **IDS-C_6**, the plane of alkyl (C_6) side chain is out of the plane of the phenyl ring with a dihedral angle of 89 degree (Figure 9), whereas the alkoxy (OC_8) side chain in **IDS-OCH_8** is positioned nearly in-plane with the phenyl ring (the dihedral angle is −1.9°, Figure 9). From the thermodynamic point of

dx.doi.org/10.1021/ma401415g | *Macromolecules* 2013, 46, 7715−7726

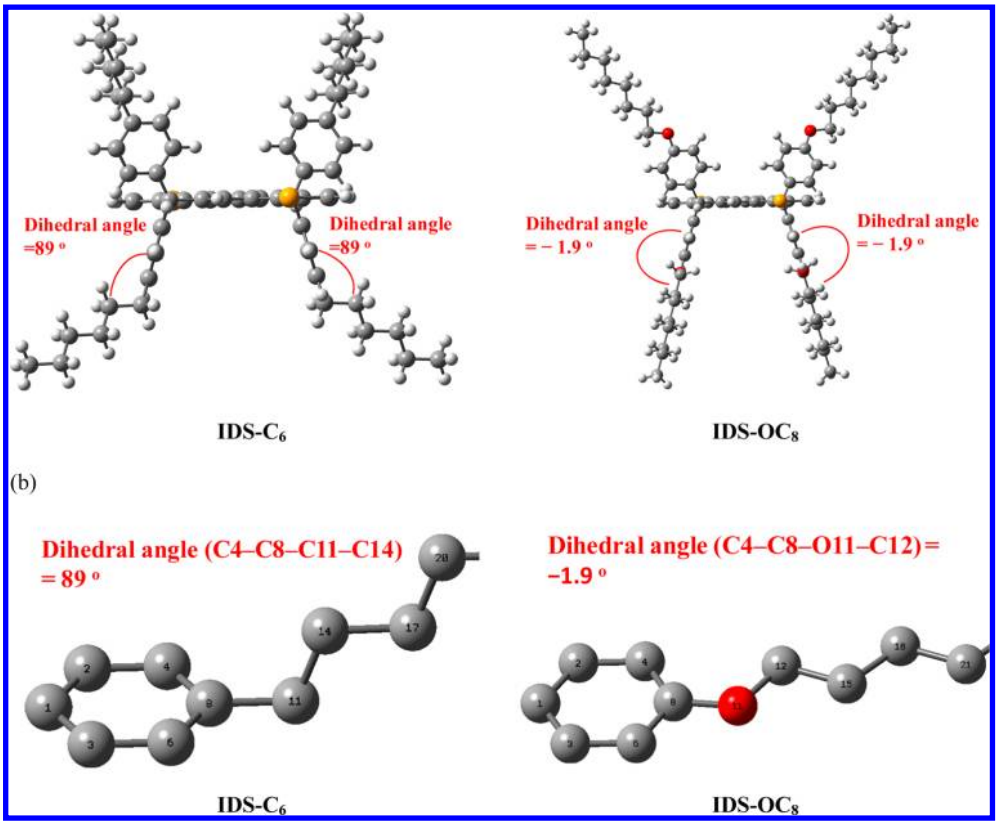

Figure 9. (a) Top view of the optimized geometries of **IDS-C$_6$** and **IDS-OCH$_8$** at the PM6 level of theory. (b) Amplified view of the dihedral angle between the alkyl/alkoxy substituent and the phenyl ring in **IDS-C$_6$** and **IDS-OCH$_8$**. Yellow: selenium. Red: oxygen. Gray: carbon. Light-gray: hydrogen.

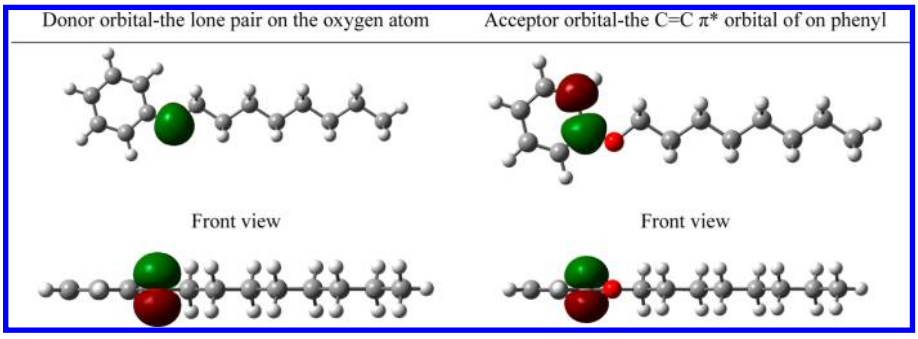

Figure 10. Plots (isovalue = 0.04 au) of the donor and acceptor orbitals involved in the interaction between the lone pair of oxygen (donor orbital) and the π^* orbital of C═C on the phenyl ring (acceptor orbital) obtained by NBO analysis, calculated at the level of B3LYP/6-311G(d,P). Red: oxygen. Gray: carbon. Light-gray: hydrogen.

view, the out-of-plane conformation (staggered, Figure 9b, left) would be lower in energy than the in-plane conformation (eclipsed, Figure 9b, right). However, the alkoxy group in **IDS-OCH$_8$** tends to adopt the eclipsed conformation with the phenyl group presumably due to the mesomeric p-π conjugation. With the intention of validating the existence of this interaction, natural bond orbital analysis (NBO) was carried out for octyloxybenzene. It reveals that an orbital interaction does exist between the lone pair of oxygen (donor orbital, Figure 10) and the π^* orbital of C═C on the phenyl ring (acceptor orbital, Figure 10) and the stabilization energy of this donor−acceptor interaction is computed to be 30.40 kcal mol^{-1}. NBO analysis of hexylbenzene was also performed, but no significant interaction was found between the phenyl ring and the alkyl chain. Consequently, the octyloxy group in **IDS-OCH$_8$** is nearly in-plane with the phenyl ring, whereas the hexyl group in **IDS-C$_6$** is out-of-plane with the phenyl ring. The steric difference between these two groups may thus result in the different molecular packing of the corresponding polymer, further affecting their photovoltaic and transistor properties. Although the side chains are substituted on the sp^3-carbon in the IDS system, the electronic and steric effects in this study would also provide useful insights for a conjugated system such as benzodithiophene unit where the alkyl or alkoxy side chains are directly attached on the conjugated backbone (sp^2-carbon).

■ CONCLUSIONS

Donor−acceptor copolymers incorporating selenophene units have emerged as promising photoactive materials because of the selenophene's unique nature to improve light-harvesting

dx.doi.org/10.1021/ma401415g | *Macromolecules* 2013, 46, 7715−7726

ability, photostability and charge mobility of the polymers. Incorporation of selenophene moiety into a ladder-type coplanar framework is of great interest in material development but synthetically less explored. In this research, we developed a new multifused pentacyclic arene, indacenodiselenophene (IDS), where the central phenylene ring is fused with two outer selenophene rings. We demonstrated that 3-position of the selenophene units can undergo Friedel−Crafts annulation which is a key step leading to the core structure of IDS. To systematically study the side-chain effect on the polymeric properties, **IDS-OCH$_8$** and **IDS-C$_6$** having 4-octyloxyphenyl and 4-hexylphenyl as the side chains were prepared, respectively. The OC$_8$ and C$_6$ side chains make negligible impact on the optical and electrochemical properties of the resulting polymers due to the fact that the side chains have no direct conjugation with the polymeric backbones. However, the solar cell performance is highly associated with the side chains of the polymers. Under similar device fabrication conditions, the **PIDSBT-C$_6$** and **PIDSFBT-C$_6$**-based devices showed much improved efficiency than the corresponding **PIDSBT-OCH$_8$**, and **PIDSFBT-OCH$_8$**-based devices (2.6% and 1.9% vs 3.8% and 3.9%). The improvement is mainly the result of much enhanced J_{sc} values. The fluorinated polymers showed the lower-lying of HOMO energy levels and thereby enhanced V_{oc}, due to the fluorine's electron-withdrawing effect on the BT unit. Consistently, **PIDSBT-C$_6$** and **PIDSFBT-C$_6$** exhibited much higher FET hole mobilites than the corresponding **PIDSBT-OCH$_8$** and **PIDSFBT-OCH$_8$**. These results revealed that the 4-hexylphenyl group is a better side chain than the 4-octyloxyphenyl group in the IDS system, and the side-chain dependent mobility of the polymers is the dominating factor to determine the J_{sc} values and efficiencies of PSCs. Theoretical calculations showed that the octyloxy group in **IDS-OCH$_8$** is nearly in-plane with the phenyl ring, whereas the hexyl group in **IDS-C$_6$** is out-of-plane with the phenyl ring. This structural variation might influence the molecular packing between the polymers. **PIDSBT-C$_6$** exhibited a highest hole mobility of 8.0 × 10^{-2} cm^2 V^{-1} s^{-1} and the **PIDSTPD-C$_6$**:$PC_{71}BM$ (1:4 in wt %)-based device with 5% chloronaphthalene (CN) exhibited a highest V_{oc} of 0.92 V, a J_{sc} of 9.77 mA/cm^2, an FF of 51%, and a highest PCE of 4.6%. This research not only reports a new selenophene-based IDS arene for PSCs but also provides useful insights into the side-chain effect for D−A conjugated copolymers.

EXPERIMENTAL SECTION

General Measurement and Characterization. All chemicals are purchased from Aldrich or Acros and used as received unless otherwise specified. ^{1}H and ^{13}C NMR spectra were measured using Varian 300 and 400 MHz instrument spectrometers. Thermogravimetric analysis (TGA) was recorded on a Perkin-Elmer Pyris under nitrogen atmosphere at a heating rate of 10 °C/min. Absorption spectra were recorded on a HP8453 UV−vis spectrophotometer. The molecular weight of polymers were measured on a Viscotek VE2001GPC, and polystyrene was used as the standard (THF as the eluent). The electrochemical cyclic voltammetry (CV) was conducted on a CH Instruments Model 611D. A carbon glass coated with a thin polymer film was used as the working electrode and Ag/Ag^+ electrode as the reference electrode, while 0.1 M tetrabutylammonium hexafluorophosphate (Bu_4NPF_6) in acetonitrile was the electrolyte. CV curves were calibrated using ferrocence as the standard, whose oxidation potential is set at −4.8 eV with respect to zero vacuum level. The HOMO energy levels were obtained from the equation HOMO = $-(E_{ox}{}^{onset} - E_{(ferrocene)}{}^{onset} + 4.8)$ eV. The LUMO levels of polymer were obtained from the equation LUMO = $-(E_{red}{}^{onset} - E_{(ferrocene)}{}^{onset} + 4.8)$ eV.

OFET Fabrication. An n-type heavily doped Si wafer with a SiO_2 layer of 325 nm and a capacitance of 10.6 nF/cm^2 was used as the gate electrode and dielectric layer. Thin films (40−60 nm in thickness) of polymers were deposited on octadecyltrichlorosilane- (ODTS-) treated SiO_2/Si substrates by spin-coating their toluene solutions (5 mg/mL). Then, the thin films were annealed at different temperatures (120 or 200 °C) for 10 min. Gold source and drain contacts (40 nm in thickness) were deposited by vacuum evaporation on the organic layer through a shadow mask, affording a bottom-gate, top-contact device configuration. Electrical measurements of OTFT devices were carried out at room temperature in air using a 4156C, Agilent Technologies. The field-effect mobility was calculated in the saturation regime by using the equation $I_{ds} = (\mu WC_i/2L)(V_g - V_t)^2$, where I_{ds} is the drain-source current, μ is the field-effect mobility, W is the channel width (1 mm), L is the channel length (100 μm), C_i is the capacitance per unit area of the gate dielectric layer, V_g is the gate voltage, and V_t is the threshold voltage.

PSCs Fabrication. ITO/glass substrates were ultrasonically cleaned sequentially in detergent, water, acetone and 2-propanol (IPA). The cleaned substrates were covered by a 30 nm thick layer of PEDOT:PSS (Clevios P 4083 provided by Stark) by spin-coating. After annealing in a glovebox at 150 °C for 30 min, the samples were cooled to room temperature. Polymers were dissolved in *o*-dichlorobenzene (ODCB), and then $PC_{71}BM$ (purchased from Lumtec) was added. The solution was then heated at 80 °C and stirred overnight at the same temperature. Prior to deposition, the solution was filtered (0.45 μm filters). The solution of polymer:$PC_{71}BM$ was then spin coated to form the active layer. The cathode made of calcium (350 nm thick) and aluminum (1000 nm thick) was sequentially evaporated through a shadow mask under high vacuum (<10^{-6} Torr). Each sample consists of 4 independent pixels defined by an active area of 0.04 cm^2. Finally, the devices were encapsulated and characterized in air.

Synthesis of 1. A mixture of diethyl 2,5-dibromoterephthalate (6.05 g, 15.9 mmol), 2-(tributylstannyl)selenophene (14.7 g, 35.0 mmol), $Pd(PPh_3)_2Cl_2$ (0.45 g, 0.64 mmol), and degassed toluene (80 mL) was heated to 130 °C under nitrogen atmosphere for 16 h. The reaction mixture was poured into water (150 mL) and extracted with ethyl acetate (250 mL × 3). The combined organic layer was dried over $MgSO_4$ and the solvent was removed *in vacuo*. The residue was purified by column chromatography on silica gel (hexane/ethyl acetate, v/v, 20/1) and then recrystallized from hexane to give a yellow solid **1** (4.7 g, 62%). ^{1}H NMR ($CDCl_3$, 400 MHz, ppm): δ 1.16 (t, J = 7.2 Hz, 6 H), 4.21 (q, J = 7.2 Hz, 4 H), 7.22−7.23 (m, 2 H), 7.3 (dd, J = 5.6, 3.6 Hz, 2 H), 7.78 (s, 2 H), 8.08−8.09 (m, 2 H). ^{13}C NMR ($CDCl_3$, 100 MHz, ppm): δ 13.7, 61.6, 129.2, 129.6, 131.7, 132.3, 133.6, 135.4, 146.3, 167.7. MS (EI, $M^{+\cdot}$, $C_{20}H_{18}O_4Se_2$): calcd, 480.27; found, 481.

Synthesis of 2. 4-Octyloxyphenyl magnesium bromide was prepared by the following procedure. To a suspension of magnesium turnings (3.2 g, 131.7 mmol) and 3−4 drops of 1,2-dibromoethane in dry THF (120 mL) was slowly added 1-bromo-4-octyloxy-benzene (34.22 g, 120.0 mmol) dropwise and the mixture was then stirred for 1 h. To a THF (50 mL) solution of **1** (4.60 g, 9.6 mmol) under nitrogen atmosphere was added dropwise the freshly prepared 4-octyloxyphenyl magnesium bromide (1 M, 76.6 mL, 76.6 mmol) at room temperature. The resulting mixture was heated at the refluxing temperature for 16 h, cooled to rt, poured into water (100 mL), and extracted with ethyl acetate (150 mL × 3). The collected organic layer was dried over $MgSO_4$. After removal of the solvent under reduced pressure, the residue was purified by column chromatography on silica gel (hexane/ethyl acetate, v/v, 30/1) to furnish a yellow solid **2** (4.7 g, 40%). ^{1}H NMR ($CDCl_3$, 400 MHz, ppm): δ 0.88, (t, J = 7 Hz, 12 H), 1.28−1.47 (m, 40 H), 1.75−1.79 (m, 8 H), 3.61 (s, 2 H), 3.94 (t, J = 6.6 Hz, 8 H), 6.47 (dd, J = 3.8, 1 Hz, 2 H), 6.75 (s, 2 H), 6.81 (dd, J = 8.8 Hz, 8 H), 6.99 (dd, J = 5.6, 3.6 Hz, 2 H), 7.07 (d, J = 8.8 Hz, 8 H), 7.89 (dd, J = 5.6, 1.2 Hz, 2 H). ^{13}C NMR ($CDCl_3$, 100 MHz, ppm): δ 14.1, 22.6, 26.0, 29.2, 29.3, 29.4, 31.8, 68.0, 82.5, 113.8, 129.1, 129.2,

dx.doi.org/10.1021/ma401415g | Macromolecules 2013, 46, 7715−7726

130.5, 133.2, 133.8, 135.9, 139.8, 144.5, 148.7, 158.3. MS (FAB, $M^{+\cdot}$, $C_{72}H_{94}O_6Se_2$): calcd, 1213.43; found, 1212.

Synthesis of IDS-OCH$_8$. To a solution of **2** (1.00 g, 0.81 mmol) in octane (100 mL) was added acetic acid (10 mL) and concentrated sulfuric acid (1 mL). The mixture was stirred for 4 h at 70 °C, cooled to room temperature, poured into water (250 mL), and extracted with ethyl acetate (500 mL × 3). The combined organic layer was dried over $MgSO_4$ and the solvent was removed under reduced pressure. The residue was then purified by column chromatography on silica gel (hexane/dichloromethane, v/v, 10/1) to afford an yellow solid **IDS-OC$_8$** (0.7 g, 73%). ^{1}H NMR ($CDCl_3$, 400 MHz, ppm): δ 0.88 (t, J = 7.2 Hz, 12 H), 1.26−1.42 (m, 40 H), 1.72−1.76 (m, 8 H), 3.90 (t, J = 6.6 Hz, 8 H), 6.76 (d, J = 8.8 Hz, 8 H), 7.14 (d, J = 8.8 Hz, 8 H), 7.17 (d, J = 5.6 Hz, 2 H), 7.35 (s, 2 H), 7.87 (d, J = 5.6 Hz, 2 H). ^{13}C NMR ($CDCl_3$, 100 MHz, ppm): δ 14.1, 22.6, 26.1, 29.2, 29.3, 29.3, 31.8, 63.1, 67.9, 114.1, 117.4, 125.5, 129.0, 132.0, 136.5, 137.4, 143.9, 153.1, 157.8, 158.0; MS (FAB, $M^{+\cdot}$, $C_{72}H_{90}O_4Se_2$): calcd, 1177.4; found, 1176.

Synthesis of Sn-IDS-OCH$_8$. To a THF (30 mL) solution of **IDS-OC$_8$** (0.74 g, 0.63 mmol) was added a hexane solution of *n*-BuLi (2.5M, 1.57 mmol) dropwise at −78 °C (liquid nitrogen/acetone bath). The mixture was stirred at this temperature for 30 min, removed from the liquid nitrogen/acetone bath, and stirred for another 30 min. A THF solution of chlorotrimethylstannane (1.0 M, 1.89 mmol) was then introduced dropwise. It was quenched with water (50 mL) and extracted with ether (50 mL × 3). The collected organic layer was dried over $MgSO_4$ and the solvent was removed *in vauco*. The residue was recrystallized from hexane to give a brown solid **Sn-IDS-OC$_8$** (0.35 g, 42%). ^{1}H NMR ($CDCl_3$, 400 MHz, ppm): δ 0.32 (s, 18 H), 0.88 (t, J = 7.2 Hz, 12 H), 1.27−1.42 (m, 40 H), 1.72−1.76 (m, 8 H), 3.90 (t, J = 6.6 Hz, 8 H), 6.76 (d, J = 8.8 Hz, 8 H), 7.14 (d, J = 8.8 Hz, 8 H), 7.25 (s, 2 H), 7.30 (s, 2 H). ^{13}C NMR ($CDCl_3$, 100 MHz, ppm): δ −7.7, 14.1, 22.6, 26.1, 29.2, 29.3, 29.3, 31.8, 62.6, 67.9, 114.1, 117.8, 129.1, 133.3, 136.9, 137.3, 148.2, 149.5, 153.4, 157.8. 159.5. MS (FAB, $M^{+\cdot}$, $C_{78}H_{106}O_4Se_2Sn_2$): calcd, 1503.01; found, 1502.

Synthesis of IDS-C$_6$. To a solution of 1-bromo-4-hexylbenzene (3.0 g, 12.5 mmol) in THF (25 mL) was added dropwise *n*-BuLi (5.5 mL, 2.5 M in hexane, 13.75 mmol) at −78 °C. The reaction mixture was stirred for 1 h and to the mixture was added a THF (15 mL) solution of compound **1** (1.0 g, 2.1 mmol). It was kept at −78 °C for 1 h, slowly warmed to room temperature, stirred overnight, then quenched with water, and extracted with ethyl acetate. The combined organic layer was dried over Na_2SO_4, filtrated, and evaporated under vacuum. The resulting white residue was then mixed with octane (100 mL) and acetic acid (10 mL). After the addition of concentrated H_2SO_4 (1 mL), the reaction was allowed to reflux for 4 h and quenched with water (100 mL). The mixture was extracted with CH_2Cl_2 and the combined organic layer was washed with water 3 times and dried over Na_2SO_4. After filtration and evaporation under reduced pressure, the resultant residue was purified by silica gel chromatography (hexane/CH_2Cl_2, v/v, 10/1) to afford a white solid **IDS-C$_6$** (1.4 g 67%). ^{1}H NMR ($CDCl_3$, 400 MHz, ppm): δ 0.88 (t, J = 6.4 Hz, 12 H), 1.27−1.33 (m, 24 H), 1.57−1.60 (m, 8 H), 2.56 (t, J = 7.8 Hz, 8 H), 7.06 (d, J = 8.2 Hz, 8 H), 7.15 (d, J = 8.2 Hz, 8 H), 7.21 (d, J = 5.4 Hz, 2 H), 7.40 (s, 2 H), 7.87 (d, J = 5.4 Hz, 2 H). ^{13}C NMR ($CDCl_3$, 100 MHz, ppm): δ 14.1, 22.6, 29.1, 31.2, 31.7, 35.6, 63.8, 117.6, 125.7, 127.9, 128.2, 131.8, 137.5, 141.3, 141.9, 144.2, 152.8, 157.4.

Synthesis of Sn-IDS-C$_6$. To a THF (30 mL) solution of **IDS-C$_6$** (1.0 g, 1.0 mmol) was added a hexane solution of *n*-BuLi (1 mL, 2.5M, 2.5 mmol) dropwise at −78 °C. The mixture was stirred at this temperature for 1 h and a THF solution of chlorotrimethylstannane (1.0 M, 3.0 mmol) was then introduced dropwise. It was quenched with water (50 mL) and extracted with ether (50 mL × 3). The collected organic layer was dried over $MgSO_4$ and the solvent was removed *in vauco*. The residue was recrystallized from hexane to give a brown solid **Sn-IDS-C$_6$** (0.84 g, 63%). ^{1}H NMR ($CDCl_3$, 400 MHz, ppm): δ 0.33 (s, 18 H), 0.87 (t, J = 6.2 Hz, 12 H), 1.29 (m, 24 H), 1.59 (m, 8 H), 2.55 (t, J = 7.8 Hz, 8 H), 7.04 (d, J = 8.2 Hz, 8 H), 7.14 (d, J = 8.2 Hz, 8 H), 7.29 (s, 2 H), 7.35 (s, 2 H). ^{13}C NMR ($CDCl_3$, 100 MHz, ppm): δ −7.7, 14.1, 22.6, 29.1, 31.3, 31.7, 35.6, 63.4, 117.9, 128.0, 128.2, 133.5, 137.3, 141.1, 142.2, 147.9, 149.7, 153.0. 159.2.

Synthesis of PIDSBT−OC$_8$. To a 50 mL round-bottom flask were introduced **Sn−IDS−OC$_8$** (200 mg, 0.133 mmol), 4,7-dibromo-2,1,3-benzothiadiazole (39.1 mg, 0.133 mmol), $Pd_2(dba)_3$ (4.6 mg, 0.005 mmol), tri(*o*-tolyl)phosphine (13.1 mg, 0.043 mmol), and dry chlorobenzene (6 mL). The mixture was bubbled with nitrogen for 10 min at room temperature. The reaction was then carried out in a microwave reactor under 270 W for 50 min. In order to end-cap the resultant polymer, tributyl(thiophen-2-yl)stannane (25.0 mg, 0.067 mmol) was added to the mixture, and the microwave reaction was continued for 10 min under 270 W. Subsequent to the addition of tributyl(thiophen-2-yl)stannane, another end-capping reagent, 2-bromothiophene (11.7 mg, 0.072 mmol), was added and the reaction was continued for another 10 min under otherwise identical conditions. The mixture was then added into methanol dropwise. The precipitate was collected by filtration and washed by Soxhlet extraction with acetone and hexane sequentially for three days. The crude polymer was dissolved in hot THF and the residual Pd catalyst and Sn metal in the THF solution was removed by Pd−thiol gel and Pd−TAAcOH (Silicycle Inc.). After filtration and removal of the solvent, the polymer was redissolved in THF and reprecipitated by methanol. The resultant polymer was collected by filtration and dried under vacuum for 1 day to afford a dark-green fiber-like solid (150 mg, 87%, M_n =10700, PDI = 1.70). ^{1}H NMR ($CDCl_3$, 400 MHz): δ 0.87 (br, 12 H), 1.26−1.42 (br, 40 H), 1.75 (br, 8 H), 3.92 (br, 8 H), 6.82 (br, 8 H), 7.25 (br, 8 H), 7.45 (br, 2 H), 7.78 (br, 2 H), 8.01 (br, 2 H).

Synthesis of PIDSFBT-OC$_8$. To a 50 mL round-bottom flask were introduced **Sn−IDS−OC8** (200 mg, 0.133 mmol), 4,7-diiodo-5,6-difluoro-2,1,3-benzothiadiazole (56.4 mg, 0.133 mmol), $Pd_2(dba)_3$ (4.6 mg, 0.005 mmol), tri(*o*-tolyl)phosphine (13.1 mg, 0.043 mmol), and dry chlorobenzene (6 mL). The mixture was bubbled with nitrogen for 10 min at room temperature. The reaction was then carried out in a microwave reactor under 270 W for 50 min. In order to end-cap the resultant polymer, tributyl(thiophen-2-yl)stannane (25.0 mg, 0.067 mmol) was added to the mixture, and the microwave reaction was continued for 10 min under 270 W. Subsequent to the addition of tributyl(thiophen-2-yl)stannane, another end-capping reagent, 2-bromothiophene (11.7 mg, 0.072 mmol), was added and the reaction was continued for another 10 min under otherwise identical conditions. The mixture was then added into methanol dropwise. The precipitate was collected by filtration and washed by Soxhlet extraction with acetone and hexane sequentially for three days. The crude polymer was dissolved in hot THF and the residual Pd catalyst and Sn metal in the THF solution was removed by Pd-thiol gel and Pd-TAAcOH (Silicycle Inc.). After filtration and removal of the solvent, the polymer was redissolved in THF and reprecipitated by methanol. The resultant polymer was collected by filtration and dried under vacuum for 1 day to afford a dark-blue fiber-like solid (156 mg, 87%, M_n = 11500, PDI = 1.70). ^{1}H NMR ($CDCl_3$, 400 MHz): δ 0.87 (br, 12 H), 1.26−1.44 (br, 40 H), 1.76 (br, 8 H), 3.92 (br, 8 H), 6.83 (br, 8 H), 7.25 (br, 8 H), 7.49 (m, 2 H), 8.38 (br, 2 H).

Synthesis of PIDSBT−C$_6$. To a 50 mL round-bottom flask were introduced **Sn−IDS−C6** (200 mg, 0.151 mmol), 4,7-dibromo-2,1,3-benzothiadiazole (44.3 mg, 0.151 mmol), $Pd_2(dba)_3$ (5.5 mg, 0.006 mmol), tri(*o*-tolyl)phosphine (14.6 mg, 0.048 mmol), and dry chlorobenzene (6 mL). The mixture was bubbled with nitrogen for 10 min at room temperature. The reaction was then carried out in a microwave reactor under 270 W for 50 min. In order to end-cap the resultant polymer, tributyl(thiophen-2-yl)stannane (28.4 mg, 0.076 mmol) was added to the mixture, and the microwave reaction was continued for 10 min under 270 W. Subsequent to the addition of tributyl(thiophen-2-yl)stannane, another end-capping reagent, 2-bromothiophene (13.4 mg, 0.082 mmol) was added and the reaction was continued for another 10 min under otherwise identical conditions. The mixture was then added into methanol dropwise. The precipitate was collected by filtration and washed by Soxhlet extraction with acetone and hexane sequentially for three days. The crude polymer was dissolved in hot THF and the residual Pd catalyst and Sn metal in the THF solution was removed by Pd−thiol gel and

dx.doi.org/10.1021/ma401415g | *Macromolecules* 2013, 46, 7715−7726

Pd−TAAcOH (Silicycle Inc.). After filtration and removal of the solvent, the polymer was redissolved in THF and reprecipitated by methanol. The resultant polymer was collected by filtration and dried under vacuum for 1 day to afford a give a dark-green fiber-like solid (163 mg, 95%, M_n =10800, PDI = 2.0). δ ^{1}H NMR ($CDCl_3$, 400 MHz): δ 0.87 (br, 12 H), 1.29−1.34 (br, 24 H), 1.60 (br, 8 H), 2.57 (br, 8 H), 7.10 (br, 8 H), 7.25 (br, 8 H), 7.47 (br, 2 H), 7.78 (br, 2 H), 8.02 (br, 2 H).

Synthesis of PIDSFBT-C_6. To a 50 mL round-bottom flask were introduced **Sn−IDS−C6** (200 mg, 0.151 mmol), 4,7-diiodo-5,6-difluoro-2,1,3-benzothiadiazole (64.0 mg, 0.151 mmol), $Pd_2(dba)_3$ (5.5 mg, 0.006 mmol), tri(*o*-tolyl)phosphine (14.7 mg, 0.048 mmol), and dry chlorobenzene (6 mL). The mixture was bubbled with nitrogen for 10 min at room temperature. The reaction was then carried out in a microwave reactor under 270 W for 50 min. In order to end-cap the resultant polymer, tributyl(thiophen-2-yl)stannane (28.4 mg, 0.076 mmol) was added to the mixture, and the microwave reaction was continued for 10 min under 270 W. Subsequent to the addition of tributyl(thiophen-2-yl)stannane, another end-capping reagent, 2-bromothiophene (13.4 mg, 0.082 mmol) was added and the reaction was continued for another 10 min under otherwise identical conditions. The mixture was then added into methanol dropwise. The precipitate was collected by filtration and washed by Soxhlet extraction with acetone and hexane sequentially for three days. The crude polymer was dissolved in hot THF and the residual Pd catalyst and Sn metal in the THF solution was removed by Pd−thiol gel and Pd−TAAcOH (Silicycle Inc.). After filtration and removal of the solvent, the polymer was redissolved in THF and reprecipitated by methanol. The resultant polymer was collected by filtration and dried under vacuum for 1 day to afford a give a dark-blue fiber-like solid (170 mg, 96%, M_n = 9300, PDI = 1.6). δ ^{1}H NMR ($CDCl_3$, 400 MHz): δ 0.87 (br, 12 H), 1.29−1.34 (br, 24 H), 1.60 (br, 8 H), 2.57 (br, 8 H), 7.10 (d, J = 8 Hz, 8 H), 7.25 (br, J = 8 Hz, 8 H), 7.51 (br, 2 H), 8.37 (br, 2 H).

Synthesis of PIDSTPD−C_6. To a 50 mL round-bottom flask were introduced **Sn−IDS−C6** (200 mg, 0.151 mmol), 1,3-dibromothieno-[3,4-*c*]pyrrole-4,6-dione (63.9 mg, 0.151 mmol), $Pd_2(dba)_3$ (5.5 mg, 0.006 mmol), tri(*o*-tolyl)phosphine (14.7 mg, 0.048 mmol), and dry chlorobenzene (6 mL). The mixture was bubbled with nitrogen for 10 min at room temperature. The reaction was then carried out in a microwave reactor under 270 W for 50 min. In order to end-cap the resultant polymer, tributyl(thiophen-2-yl)stannane (28.4 mg, 0.076 mmol) was added to the mixture, and the microwave reaction was continued for 10 min under 270 W. Subsequent to the addition of tributyl(thiophen-2-yl)stannane, another end-capping reagent, 2-bromothiophene (13.4 mg, 0.082 mmol) was added and the reaction was continued for another 10 min under otherwise identical conditions. The mixture was then added into methanol dropwise. The precipitate was collected by filtration and washed by Soxhlet extraction with acetone and hexane sequentially for 3 days. The crude polymer was dissolved in hot THF and the residual Pd catalyst and Sn metal in the THF solution was removed by Pd−thiol gel and Pd−TAAcOH (Silicycle Inc.). After filtration and removal of the solvent, the polymer was redissolved in THF and reprecipitated by methanol. The resultant polymer was collected by filtration and dried under vacuum for 1 day to afford a give a dark-purple fiber-like solid (177 mg, 93%). δ ^{1}H NMR ($CDCl_3$, 400 MHz): δ 0.87 (br, 15 H), 1.30 (br, 36 H), 1.59 (br, 8 H), 2.57 (br, 8 H,), 3.62 (br, 2 H,), 7.08 (br, 8 H), 7.14 (br, 8 H), 7.40 (br, 2 H), 7.66 (br, 2 H).

■ ASSOCIATED CONTENT

Supporting Information

AFM measurements, computational details, and ^{1}H and ^{13}C NMR spectra of the new compounds and copolymers. This material is available free of charge via the Internet at http://pubs.acs.org/.

■ AUTHOR INFORMATION

Corresponding Author

*E-mail: (Y.-J.C.) yjcheng@mail.nctu.edu.tw.

Notes

The authors declare no competing financial interest.

■ ACKNOWLEDGMENTS

We thank the National Science Council and the "ATU Program" of the Ministry of Education, Taiwan, for financial support. We are also grateful to the National Center for High-performance Computing (NCHC) in Taiwan for computer time and facilities.

■ REFERENCES

(1) Yu, G.; Gao, J.; Hummelen, J. C.; Wudl, F.; Heeger, A. J. *Science* **1995**, *270*, 1789.

(2) (a) Thompson, B. C.; Fréchet, J. M. J. *Angew. Chem., Int. Ed.* **2008**, *47*, 58. (b) Cheng, Y.-J.; Yang, S.-H.; Hsu, C.-S. *Chem. Rev.* **2009**, *109*, 5868. (c) Chen, J.; Cao, Y. *Acc. Chem. Res.* **2009**, *42*, 1709. (d) Li, Y.; Zou, Y. *Adv. Mater.* **2008**, *20*, 2952. (e) Li, Y. *Acc. Chem. Res.* **2012**, *45*, 723. (f) Huo, L.; Hou, J. *Polym. Chem.* **2011**, *2*, 2453. (g) Duan, C.; Huang, F.; Cao, Y. *J. Mater. Chem.* **2012**, *22*, 10416. (h) Zhou, H.; Yang, L.; You, W. *Macromolecules* **2012**, *45*, 607.

(3) (a) Svensson, M.; Zhang, F.; Veenstra, S. C.; Verhees, W. J. H.; Hummelen, J. C.; Kroon, J. M.; Inganäs, O.; Andersson, M. R. *Adv. Mater.* **2003**, *15*, 988. (b) Zhou, Q.; Hou, Q.; Zheng, L.; Deng, X.; Yu, G.; Cao, Y. *Appl. Phys. Lett.* **2004**, *84*, 1653. (c) Zhang, F.; Mammo, W.; Andersson, L. M.; Admassie, S.; Andersson, M. R.; Inganäs, O. *Adv. Mater.* **2006**, *18*, 2169. (d) Zhang, F.; Bijleveld, J.; Perzon, E.; Tvingstedt, K.; Barrau, S.; Inganäs, O.; Andersson, M. R. *J. Mater. Chem.* **2008**, *18*, 5468. (e) Schulz, G. L.; Chen, X.; Holdcroft, S. *Appl. Phys. Lett.* **2009**, *94*, 023302. (f) Huang, F.; Chen, K.-S.; Yip, H.-L.; Hau, S. K.; Acton, O.; Zhang, Y.; Luo, J.; Jen, A. K.-Y. *J. Am. Chem. Soc.* **2009**, *131*, 13886.

(4) (a) Zhu, Z.; Waller, D.; Gaudiana, R.; Morana, M.; Mühlbacher, D.; Scharber, M.; Brabec, C. *Macromolecules* **2007**, *40*, 1981. (b) Mühlbacher, D.; Scharber, M.; Zhengguo, M. M.; Zhu, M. M. Z.; Waller, D.; Gaudiana, R.; Brabec, C. *Adv. Mater.* **2006**, *18*, 2884. (c) Kim, J. Y.; Lee, K.; Coates, N. E.; Moses, D.; Nguyen, T.-Q.; Dante, M.; Heeger, A. J. *Science* **2007**, *317*, 222. (d) Peet, J.; Kim, J. Y.; Coates, N. E.; Ma, W. L.; Moses, D.; Heeger, A. J.; Bazan, G. C. *Nat. Mater.* **2007**, *6*, 497. (e) Chen, C.-H.; Hsieh, C.-H.; Dubosc, M.; Cheng, Y.-J.; Hsu, C.-S. *Macromolecules* **2010**, *43*, 697.

(5) (a) Liang, Y.; Wu, Y.; Feng, D.; Tsai, S.-T.; Son, H.-J.; Li, G.; Yu, L. *J. Am. Chem. Soc.* **2009**, *131*, 56. (b) He, F.; Wang, W.; Chen, W.; Xu, T.; Darling, S. B.; Strzalka, J.; Liu, Y.; Yu, L. *J. Am. Chem. Soc.* **2011**, *133*, 3284. (c) Zhang, Y.; Zou, J.; Yip, H.-L.; Chen, K.-S.; Zeigler, D. F.; Sun, Y.; Jen, A. K.-Y. *Chem. Mater.* **2011**, *23*, 2289. (d) Wu, J.-S.; Cheng, Y.-J.; Dubosc, M.; Hsieh, C.-H.; Chang, C.-Y.; Hsu, C.-S. *Chem. Commun.* **2010**, *46*, 3259. (e) Wu, J.-S.; Cheng, Y.-J.; Lin, T.-Y.; Chang, C.-Y.; Shih, P.-I.; Hsu, C.-S. *Adv. Funct. Mater.* **2012**, *22*, 1711. (f) Wang, J.-Y.; Hau, S. K.; Yip, H.-L.; Davies, J. A.; Chen, K.-S.; Zhang, Y.; Sun, Y.; Jen, A. K.-Y. *Chem. Mater.* **2011**, *23*, 765. (g) Ashraf, R. S.; Chen, Z.; Leem, D. S.; Bronstein, H.; Zhang, W.; Schroeder, B.; Geerts, Y.; Smith, J.; Watkins, S.; Anthopoulos, T. D.; Sirringhaus, H.; Mello, J. C. de; Heeney, M.; McCulloch, I. *Chem. Mater.* **2011**, *23*, 768. (h) Zhang, M.; Guo, X.; Wang, X.; Wang, H.; Li, Y. *Chem. Mater.* **2011**, *23*, 4264. (i) Cheng, Y.-J.; Ho, Y.-J.; Chen, C.-H.; Kao, W.-S.; Wu, C.-E.; Hsu, S.-L.; Hsu, C.-S. *Macromolecules* **2012**, *45*, 2690. (j) Zhang, Y.; Zou, J.; Yip, H.-L.; Chen, K.-S.; Davies, J. A.; Sun, Y.; Jen, A. K. Y. *Macromolecules* **2011**, *44*, 4752.

(6) (a) Goldfinger, M. B.; Crawford, K. B.; Swager, T. M. *J. Am. Chem. Soc.* **1997**, *119*, 4578. (b) Goldfinger, M. B.; Swager, T. M. *J. Am. Chem. Soc.* **1994**, *116*, 7895. (c) Forster, M.; Annan, K. O.; Scherf, U. *Macromolecule* **1999**, *32*, 3159. (d) Scherf, U. *J. Mater. Chem.* **1999**, *9*, 1853. (d) Chmil, K.; Scherf, U. *Acta Polym.* **1997**, *48*, 208. (e) Jacob, J.; Sax, S.; Piok, T.; List, E. J. W.; Grimsdale, A. C.; Mullen, K. *J. Am.*

Chem. Soc. **2004**, *126*, 6987. (f) Zheng, Q.; Jung, B. J.; Sun, J.; Katz, H. E. *J. Am. Chem. Soc.* **2010**, *132*, 5394. (g) Facchetti, A. *Chem. Mater.* **2011**, *23*, 733. (h) Guo, X.; Ortiz, R. P.; Zheng, Y.; Hu, Y.; Noh, Y.-Y.; Baeg, K.-J.; Facchetti, A.; Marks, T. J. *J. Am. Chem. Soc.* **2011**, *133*, 1405. (i) Cheng, Y.-J.; Ho, Y.-J.; Chen, C.-H.; Kao, W.-S.; Wu, C.-E.; Hsu, S.-L.; Hsu, C.-S. *Macromolecules* **2012**, *45*, 2690. (j) Cheng, Y.-J.; Cheng, S.-W.; Chang, C.-Y.; Kao, W.-S.; Liao, M.-H.; Hsu, C.-S. *Chem. Commun.* **2012**, *48*, 3203.

(7) (a) Chen, C.-H.; Cheng, Y.-J.; Dubosc, M.; Hsieh, C.-H.; Chu, C.-C.; Hsu, C.-S. *Chem. Asian. J.* **2010**, *5*, 2480. (b) Cheng, Y.-J.; Chen, C.-H.; Lin, Y.-S.; Chang, C.-Y.; Hsu, C.-S. *Chem. Mater.* **2011**, *23*, 5068. (c) Chen, C.-H.; Cheng, Y.-J.; Chang, C.-Y.; Hsu, C.-S. *Macromolecules* **2011**, *44*, 8415. (d) Chen, Y.-C.; Yu, C. -Y.; Fan, Y.-L.; Huang, L.-I.; Chen, C.-P.; Ting, C. *Chem. Commun.* **2010**, *46*, 6503. (e) Chen, C.-P.; Chan, S.-H.; Chao, T.-C.; Ting, C.; Ko, B.-T. *J. Am. Chem. Soc.* **2008**, *130*, 12828.

(8) (a) Ballantyne, A. M.; Chen, L. C.; Nelson, J.; Bradley, D. D. C.; Astuti, Y.; Maurano, A.; Shuttle, C. G.; Durrant, J. R.; Heeney, M.; Duffy, W.; McCulloch, I. *Adv. Mater.* **2007**, *19*, 4544. (b) Chen, Z. Y.; Lemke, H.; Albert-Seifried, S.; Caironi, M.; Nielsen, M. M.; Heeney, M.; Zhang, W. M.; McCulloch, I.; Sirringhaus, H. *Adv. Mater.* **2010**, *22*, 2371. (c) Lee, W. H.; Son, S. K.; Kim, K.; Lee, S. K.; Shin, W. S.; Moon, S.; Kang, I. N. *Macromolecules* **2012**, *45*, 1303. (e) Khim, D.; Lee, W. H.; Baeg, K. J.; Kim, D. Y.; Kang, I. N.; Noh, Y. Y. *J. Mater. Chem.* **2012**, *22*, 12774. (f) Haid, S.; Mishra, A.; Uhrich, C.; Pfeiffer, M.; Bäuerle, P. *Chem. Mater.* **2011**, *23*, 4435. (g) Beaupre, S.; Pron, A.; Drouin, S. H.; Najari, A.; Mercier, L. G.; Robitaille, A.; Leclerc, M. *Macromolecules* **2012**, *45*, 6906. (i) Al-Hashimi, M.; Baklar, M. A.; Colleaux, F.; Watkins, S. E.; Anthopoulos, T. D.; Stingelin, N.; Heeney, M. *Macromolecules* **2011**, *44*, 5194. (j) Nakano, M.; Mori, H.; Shinamura, S.; Takimiya, K. *Chem. Mater.* **2012**, *24*, 190. Gao, D.; Hollinger, J.; Seferos, D. S. *ACS Nano* **2012**, *6*, 7114.

(9) Zade, S. S.; Zamoshchik, N.; Bendikov, M. *Chem.—Eur. J.* **2009**, *15*, 8613.

(10) Heeney, M.; Zhang, W.; Crouch, D. J.; Chabinyc, M. L.; Gordeyev, S.; Hamilton, R.; Higgins, S. J.; McCulloch, I.; Skabara, P. J.; Sparrowe, D.; Tierney, S. *Chem. Commun.* **2007**, *43*, 5061.

(11) Saadeh, H. A.; Lu, L.; He, F.; Bullock, J. E.; Wang, W.; Carsten, B.; Yu, L. *ACS Macro Lett.* **2012**, *1*, 361.

(12) Cheng, Y.-J.; Wu, J.-S.; Shih, P.-I.; Chang, C.-Y.; Jwo, P.-C.; Kao, W.-S.; Hsu, C.-S. *Chem. Mater.* **2011**, *23*, 2361. Chang, C.-Y.; Cheng, Y.-J.; Hung, S.-H.; Wu, J.-S.; Kao, W.-S.; Lee, C.-H.; Hsu, C.-S. *Adv. Mater.* **2012**, *24*, 549. Bronstein, H.; Leem, D. S.; Hamilton, R.; Woebkenberg, P.; King, S.; Zhang, W.; Ashraf, R. S.; Heeney, M.; Anthopoulos, T. D.; de Mello, J.; McCulloch, I. *Macromolecules* **2011**, *44*, 6649. Mei, J.; Kim, D. H.; Ayzner, A. L.; Toney, M. F.; Bao, Z. *J. Am. Chem. Soc.* **2011**, *133*, 20130. Price, S. C.; Stuart, A. C.; You, W. *Macromolecules* **2010**, *43*, 4609. Zhou, H.; Yang, L.; Xiao, S.; Liu, S.; You, W. *Macromolecules* **2010**, *43*, 811. Zhang, W.; Smith, J.; Watkins, S. E.; Gysel, R.; McGehee, M.; Salleo, A.; Kirkpatrick, J.; Ashraf, S.; Anthopoulos, T.; Heeney, M.; McCulloch, I. *J. Am. Chem. Soc.* **2010**, *132*, 11437.

(13) (a) Braunecker, W. A.; Owczarczyk, Z. R.; Garcia, A.; Kopidakis, N.; Larsen, R. E.; Hammond, S. R.; Ginley, D. S.; Olson, D. C. *Chem. Mater.* **2012**, *24*, 1346. (b) Liang, Y.; Feng, D.; Wu, Y.; Tsai, S.-T.; Li, G.; Ray, C.; Yu, L. *J. Am. Chem. Soc.* **2009**, *131*, 7792. (c) Duan, R. M.; Ye, L.; Guo, X.; Huang, Y.; Wang, P.; Zhang, S. Q.; Zhang, J. P.; Huo, L. J.; Hou, J. H. *Macromolecules* **2012**, *45*, 3032. (d) Hou, J.; Chen, H.-Y.; Zhang, S.; Yang, Y. *J. Phys. Chem. C.* **2009**, *113*, 21202. (e) Huo, L.; Ye, L.; Wu, Y.; Li, Z.; Guo, X.; Zhang, M.; Zhang, S.; Hou, J. *Macromolecules* **2012**, *45*, 6923. (f) Huo, L. J.; Zhang, S. Q.; Guo, X.; Xu, F.; Li, Y. F.; Hou, J. H. *Angew. Chem., Int. Ed.* **2011**, *50*, 9697.

(14) (a) Xu, Y.-X.; Chueh, C.-C.; Yip, H.-L.; Ding, F.-Z.; Li, Y.-X.; Li, C.-Z.; Li, X.; Chen, W.-C.; Jen, A. K.-Y. *Adv. Mater.* **2012**, *24*, 6356. (b) Chang, H.-H.; Tsai, C.-E.; Lai, Y.-Y.; Chiou, D.-Y.; Hsu, S.-L.; Hsu, C.-S.; Cheng, Y.-J. *Macromolecules* **2012**, *45*, 9282.

(15) (a) Zhang, Y.; Chien, S.-C.; Chen, K.-S.; Yip, H.-L.; Sun, Y.; Davies, J. A.; Chen, F.-C.; Jen, A. K. Y. *Chem. Commun.* **2011**, *47*, 11026. (b) Zhou, H.; Yang, L.; Stuart, A. C.; Price, S. C.; Liu, S.; You, W. *Angew. Chem., Int. Ed.* **2011**, *50*, 2995. (c) Schroeder, B. C.; Huang, Z.; Ashraf, R. S.; Smith, J.; D'Angelo, P.; Watkins, S. E.; Anthopoulos, T. D.; Durrant, J. R.; McCulloch, I. *Adv. Funct. Mater.* **2012**, *22*, 1663. (d) Li, Z.; Lu, J.; Tse, S.-C.; Zhou, J.; Du, X.; Tao, Y.; Ding, J. *J. Mater. Chem.* **2011**, *21*, 3226.

(16) (a) Stewart, J. J. P. *J. Mol. Model* **2007**, *13*, 1173. (b) Puzyn, T.; Suzuki, N.; Haranczyk, M.; Rak, J. *J. Chem. Inf. Model.* **2008**, *48*, 1174.